Comparison of Analytical and CFD Modelling of the Wake Interactions of Tidal Turbines

GEBRESLASSIE, Mulualem Gebregiorgis <http://orcid.org/0000-0002-5509-5866>, BELMONT, Michael and TABOR, Gavin

Comparison of Analytical and CFD Modelling of the Wake Interactions of Tidal Turbines

Mulualem G. Gebreslassie
E-mail: mgg204@exeter.ac.uk

Michael R. Belmont
E-mail: m.r.belmont@exeter.ac.uk

Gavin R. Tabor
E-mail: g.r.tabor@exeter.ac.uk

College of Engineering, Mathematics and Physical Sciences, University of Exeter, North Park Road, Exeter, EX4 4QF, UK

***Abstract*—The status of marine current tidal energy technology is currently in the research and development phase, with a few deployments and tests of prototypes under-way in some countries. There is huge pressure for tidal farms to be of GW scale in order to have a real, economically viable impact on renewable energy utilization targets outlined for 2020. A route to achieving this is the large scale energy farm philosophy, similar to wind farms, based on very large numbers of unit current tidal stream devices. However, this in-mature technology development raises different research questions which lead to further problems in the practical implementation of tidal stream devices. Thus, the aim of the work described in this paper was (i) to formulate simplified parameterised analytic models of individual and clusters of tidal stream devices using the concept of linear momentum actuator disc theory, (ii) to perform a detailed calculations of the flow field of multiple turbines using the developed models, and (iii) to compare the analytic model results with the results calculated using a CFD based *Immersed Body Force* (IBF) model. This study has been mainly focused on a new device, Momentum-Reversal-Lift (MRL), which is a cross flow type of tidal turbine developed by Aquascientific Ltd.**

Several analytic models have been developed to describe the flow characteristics downstream of the turbine, i.e. the wake velocity profile and to estimate the total power extraction from a tidal stream farm containing ideally tenth and hundreds of devices. The developed models showed the capability to examine the wake characteristics and to estimate the performance of clusters of turbines taking in to consideration the influence of turbine to turbine interactions. A small longitudinal spacing between turbines inflicted a massive energy shadowing that affects the performance of downstream turbines. Based on the analysis of the influence of wake interaction, more than 91% of the performance of an isolated turbine can be achieved with turbines spaced 20D apart. In addition, comparison of the wake velocity profiles and the power extraction calculated using both the analytic and CFD models showed reasonable agreement.

***Index Terms*—MRL, Analytic model, Wake interaction, Power extraction**

I. Introduction

The status of marine current tidal energy technology is currently in the research and development phase, with a few deployments and tests of prototypes under-way in some countries. This emerging technology development raises different research questions which lead to further problems in the practical implementation of tidal stream devices. There is a huge pressure for tidal farms to be of GW scale in order to have a real, economically viable impact on renewable energy utilization targets outlined for 2020. A route to achieving this is the large scale energy farm philosophy, similar to wind farms, based on very large numbers of unit current tidal stream devices. However, there is still a gap in optimizing tidal stream farm designs to tackle the problem which arises due to the presence of several hundred tidal stream devices which inevitably introduces turbine to turbine interaction.

The application focus of this study is a new generation of horizontally operating device, the Momentum-Riversal-Lift (MRL) turbine, aimed at deployment primarily as block farms, rather than fences, in shallow estuaries with medium flow such as the Severn. Analytical and computational techniques have been used for many years to minimise the cost of experiments and have shown good success in supporting the design and development of new devices. The analytical and computational studies are often validated by small scale experiments in order to use them for testing ideas in a large scale prior to implementation.

Analytical methods have been used in the study of a single and clusters of tidal turbines to understand the limit of their power extraction as documented by [1–7]. A theoretical model has also been developed by [8] to explore the efficiency of arrays of turbines partially blocking a wide channel. These analytical studies have been mainly focused on a single turbine or turbines configured in the spanwise direction and lacks addressing the impact of wake interaction on downstream turbines.

In addition, CFD tools have been commonly used to support the development of tidal turbines by testing new ideas prior to implementation [9]. It is a useful tool for predicting the flow characteristics, the impact of the surrounding environment and the supporting structure on the performance of the device [10]. In general, CFD tools can investigate different issues related to tidal turbines with low cost compared to experimental studies [11], but the computational cost is still higher than the analytical approach. For a single turbine simulations, it is possible to employ more detailed CFD modelling techniques as the computational demand is manageable with the current computational resources. As the number of devices increases, such as the study of arrays of devices, the computational cost significantly increases.

Thus most researchers employ moderate cost techniques such as the actuator disc method to investigate the wake interactions in arrays of turbines. Reference [12] used a blade

element and actuator disc method to study the wake interaction of a tidal stream farm with 5 rows of turbines configured in the streamwise direction. This study showed that the power coefficient of the second row was lower than the rest of the devices due to huge wake interaction from the first row but the turbines from the third row onwards showed better power coefficients due to fast wake recovery within the array. Study of a staggered configuration of arrays of devices by [13–15] showed an acceleration of the bypass flows due to the venturi created by the turbines which could improve the performance of any downstream devices.

Experimental study of arrays of devices have been carried out by [16, 17] and they showed that with a particular inter-turbine spacing there is a potential of accelerated flow regions which can be used for high power production by deploying turbines on those regions. They have suggested that an off-set or staggered configuration would provide a better option and allows a longitudinally closely packed devices to be deployed with less wake interaction and possibly higher power extraction due to accelerated bypass flow.

Different configurations of devices were also studied by [18] using CFD and experiments and the results showed high influence of wake interaction on downstream devices if an appropriate longitudinal spacing between the rows is not used.

For economically viable tidal stream farms containing possibly hundreds of devices even these simplified CFD methods become unrealistic for task such as obtaining the individual turbine locations and loading factors. One approach to overcoming the computational barrier is the use of simplified analytic models for the farm, then embed these into a large scale computational model at the global fluid problem, e.g a farm embedded in a tidal estuary. Such simplified analytic models are frequently used for propeller wind turbines.

Thus the aim of the work described in this paper is to formulate simplified parametrised analytic models that considers the influence of wake interaction on the flow features and power extraction of the MRL turbine and to compare with the results from CFD approach. Computational studies at individual and small clusters of turbines are exploited in order to advice on various issues in the analytic models building process.

II. Methodology

A. Analytical Modelling

The application of Linear Momentum Actuator Disc Theory (LMADT) [19] to a tidal turbine in an open channel has been widely developed in recent years considering a constrained flows. To simplify the analytical modelling, the conventional axial flow tidal turbine is often assumed as a very thin circular disc of permeable membrane by several researchers where fluid flows through and around it. The fluid flow is assumed to be one dimensional in the X- direction considering the cross flow velocities to be negligible as presented by [2]. Since the turbine acts as a drag force, the fluid flow along the control volume slows as it flows through the turbine. As a result, the local area on the downstream side of the turbine expands in all direction forming a cylindrical trace of streamlines to satisfy the conservation of mass.

A recent development of the extension of LMADT analysis to a tidal turbine constrained in a fluid flow between two rigid surfaces is presented by [1], though it could not address the deformation of the free surface immediately downstream of the turbine. The analysis by [1] was later modified by [2] to account for the deformation of the free surface and this analysis can be applicable for a transverse array of turbines closely spaced but stopped short of analysing the energy loss during the mixing of the flow downstream of the turbine. The deformation has also been observed by [20] during an experiment involving a horizontal axis marine current turbine represented by a rotor disc. Reference [3] expanded the analysis to take into consideration the inevitable downstream mixing effect and successfully developed a parametrised equation to estimate the energy loss in the mixing zone. The researchers have introduced a blockage ratio to account for the blockage effect of turbines configured in the span-wise direction (transverse array of turbines).

However, to our knowledge, the impact of turbine to turbine interactions on the performance of downstream turbines has not been addressed, and it has been the focus of this study to consider these interactions in the development of analytic models. The principles used by [3] to develop the analytic models for a single row of turbines were adapted in this study and have been used as a guide for the development of parametrised analytic models taking into account the wake interactions between turbines. Fig. 1a shows a vertical plane of a channel containing a single column of n turbines in the stream-wise direction. The sketch also shows the labels of each station used for the development of the analytic models. Fig. 1b shows a horizontal plane of a channel sliced along the centre of n by m number of turbines in a tidal stream farm. The farm contains a regularly configured turbines of two rows and three columns.

The stations are mainly defined in-terms of velocity coefficients and the velocity at the inlet. β and $\beta^{'}$ represent the bypass velocity coefficients at different stations. γ represents the velocity coefficient within the turbine housing. The downstream velocity coefficient, α, represents the velocity profile in the wake of a turbine and α_{min} is the minimum value of α in the wake region. The following assumptions have been made to simplify the complexity of the problem:

- The bypass velocity coefficient all around the turbine housing is assumed equal.
- The velocities immediately upstream and downstream of each turbine are assumed as equal.
- A hydrostatic pressure was assumed at stations 11, 14, 1'4, and 24 shown in Fig. 1a
- The MRL turbine is modelled as a thin rectangular plate through which the fluid flow passes.

1) Velocity Coefficients: Wake models have been extensively developed and used for investigating the wake of wind turbines. They have been first introduced by [19, 21] and subsequently ratified and improved to consider different

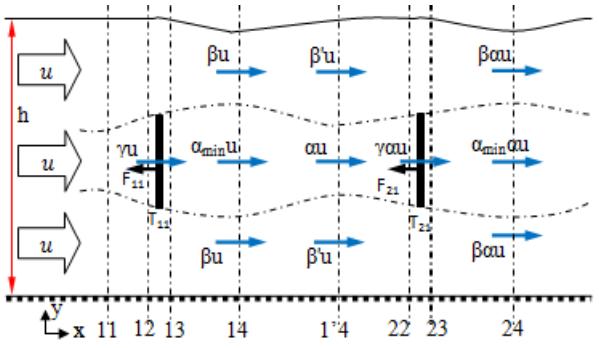

(a) Vertical plane

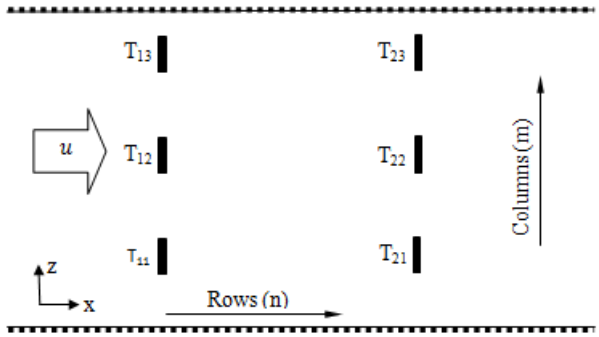

(b) Horizontal plane

Fig. 1: Sketch and notation of tidal turbine model in an open channel section

constraints by several researchers [22–25]. A commonly used wake model in the investigation of the wake characteristics of wind turbines was developed by [23, 24], but excludes the near turbine region of the wake. This wake model has been adapted in this study to represent the recovering region given in Fig. 2.

The wake of a tidal turbine has complex flow features and depends on the loading of the turbine. In this study, the wake profile is represented by $\alpha(x)$ function. This function has several minima and maxima points if the flow is turbulent and helps to define the velocity profile on the downstream of any turbine which can be described as:

$$u_d(x) = \alpha(x)u \tag{1}$$

where, $u_d(x)$ is the downstream velocity profile which is represented by $u_N(x)$ and $u_R(x)$ in the near turbine and recovering regions respectively as shown in Fig. 2. The function can be defined in terms of the mixing length and/or the spacing between turbines, x , as:

$$\alpha = \overline{f}(x, P_m) \tag{2}$$

where: P_m is set of M parameters. The velocity coefficient values should be within the range $\alpha_{min} < \gamma < 1$ and $\alpha(x) \leq 1$. This $\alpha(x)$ function can be termed as wake velocity coefficient as it defines the velocity profile at the wake region. The wake region is affected by two processes. The first process occurs in the near turbine region where the velocity value decreases and the second process occurs in the recovering region where the velocity recovers back to its initial condition. Fig. 2 shows these two processes and the wake velocity coefficient function has been developed based on this Figure. The near turbine region covers a very small distance

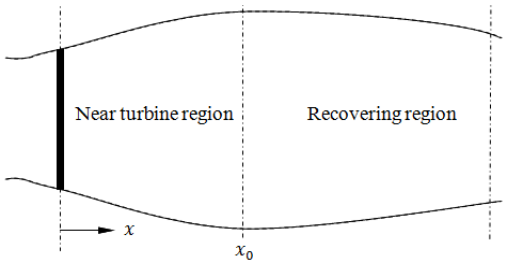

Fig. 2: Schematic representation of the Near turbine and recovering processes regions

downstream of the turbine until the point where the minimum velocity occurs. The recovering region, which starts from the minimum velocity, covers the rest of the wake region until the downstream turbine.

The near turbine region has been excluded by several researches in the investigation of the wake characteristics of wind turbines. However, it is important to include this region so that the wake velocity profile of the whole wake region can be fully understood. The wake model is derived from the concept of conservation of mass across a control volume in the near turbine region as shown in Fig. 3. Assuming that

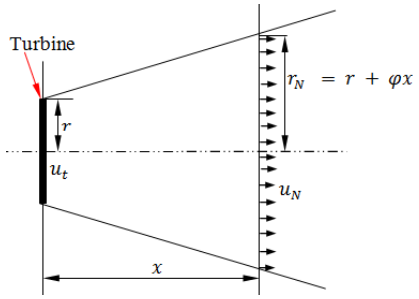

Fig. 3: Schematic representation of the wake region near the turbine

the momentum is conserved in the near turbine region and applying the continuity equation on the control volume shown in Fig. 3, the continuity equation of the near turbine region is written as:

$$Au_t = A_N(x)u_N(x) \tag{3}$$

where:$u_N(x)$ is the velocity at the near turbine region, A is the swept area of the turbine, $A_N(x)$ is the expanded area downstream of the turbine in the near turbine region, $u_t = \gamma u$ is the velocity at the turbine. The MRL turbine is a cross flow type of tidal turbine and the swept area is calculated considering its length and diameter. Therefore, area of the turbine, A , can be defined as:

$$A = 2Lr \tag{4}$$

and the area of the expanding wake can be defined as:

$$A_N(x) = 2Lr_N \tag{5}$$

where: r is half of the diameter ($r = D/2$), r_N is half of the diameter of the expanding wake as shown in Fig. 3, and L is length of the turbine. It is assumed that the wake expands linearly and the radius of this expanding wake can be defined as:

$$r_N = r + \varphi x \tag{6}$$

where: x is the mixing length scale and/or the spacing between the turbines, and φ is the wake spreading or entrainment constant. Thus, substituting these variables in Equation 3 and solving for the value of $u_N(x)$, the wake model equation can be written as:

$$u_N(x) = u\left(\frac{\gamma}{1+\varphi\frac{x}{r}}\right) \tag{7}$$

Combining Equations 1 and 7, the wake velocity coefficient function ($\alpha_N(x)$) in the near turbine region can be written as:

$$\alpha_N(x) = \frac{\gamma}{1+\varphi\frac{x}{r}} \tag{8}$$

The recovering region is the second region of the wake of the turbine. Fig. 4 shows the wake model, which has been widely used by several researchers in the wind energy technology. The schematic diagrams of the near turbine and recovering regions appears to be contradicting as both start at the turbine with different velocity values (u_{min} and u_t). However, in order to simplify the problem the near turbine region has been assumed negligible in the development of the wake velocity profile for the recovering region and this region has been represented by the wake model developed for wind turbines by [23, 24]. Assuming that the momentum is

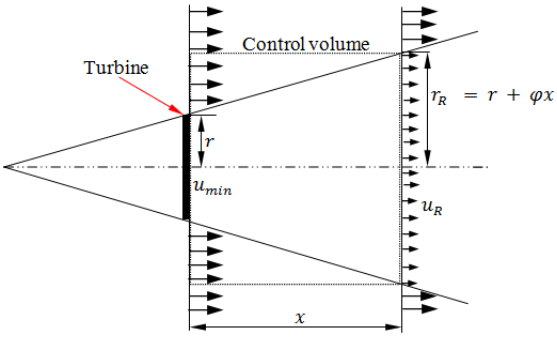

Fig. 4: Schematic wake model of the recovering region

conserved in the wake region shown in Fig. 4, the continuity equation at the inlet and outlet of the control volume is written as:

$$Au_{min} + (A_R(x) - A)u = A_R(x)u_R(x) \tag{9}$$

where: u_{min} is the minimum velocity at a distance of x_0 downstream of the turbine, $u_R(x)$ is the velocity profile in the recovering region, $A_R(x)$ is the expanding area in the recovering region given as $A_R(x) = 2Lr_R$. According to the Betz theory, the minimum velocity downstream of a turbine is given as $u_{min} = (1-2a)\,u$ where $a = (1-\gamma)$. Thus, substituting these variables in Equation 9 and solving for the value of $u_R(x)$, the wake model of the recovering process can be written as:

$$u_R(x) = u\left(1 - \frac{2\,(1-\gamma)}{1+\varphi\frac{x-x_0}{r}}\right) \tag{10}$$

As $x \Rightarrow \infty, u_R(x) \Rightarrow u$. Equation 10 is a definition of the wake model for any upstream turbine. However, in order to define the wake model of several rows of turbines in a tidal stream farm, the above equation can be easily modified taking into consideration the effect of wake interaction on the downstream turbines. The wake model downstream of the second row of the turbines is therefore defined as:

$$u_{2R} = u\left(1 - \frac{2\,(1-\gamma)}{1+\varphi\frac{x-x_0}{r}}\right)\left(1 - \frac{2\,(1-\gamma)}{1+\varphi\frac{x_{max}-x_0}{r}}\right) \tag{11}$$

Similarly for n turbines, the wake velocity profile of the n^{th} turbine in the recovering region can be defined as:

$$u_{nR} = u\left(1 - \frac{2\,(1-\gamma)}{1+\varphi\frac{x-x_0}{r}}\right)\left(1 - \frac{2\,(1-\gamma)}{1+\varphi\frac{x_{max}-x_0}{r}}\right)^{(n-1)} \tag{12}$$

where, x_{max} is the maximum mixing length or turbine spacing. The outlet velocity of upstream turbine at the maximum turbine spacing is used as an inlet to the downstream turbine. This is why the multiplying factor in Equations 11 and 12 should be calculated at the maximum turbine spacing. Combining Equations 1 and 10, the wake velocity coefficient of a single turbine in the recovering region can be written as:

$$\alpha_R(x) = 1 - \frac{2\,(1-\gamma)}{1+\varphi\frac{x-x_0}{r}} \tag{13}$$

Similarly, the wake velocity coefficient of the n^{th} turbine can be defined as:

$$\alpha_R(x) = \left(1 - \frac{2\,(1-\gamma)}{1+\varphi\frac{x-x_0}{r}}\right)\left(1 - \frac{2\,(1-\gamma)}{1+\varphi\frac{x_{max}-x_0}{r}}\right)^{(n-1)} \tag{14}$$

Based on the analytic models developed for the two regions, a combined equation that can define the wake region of the two processes given in Fig. 2 can be formulated using a transition point where the minimum velocity occurs ($u_d(x) = u_N(x) = u_R(x)$). At the transition point, the downstream distance from the turbine is considered as x_0. This distance can be obtained empirically by combining Equations 8 and 13, and with some manipulation, it can be written as:

$$x_0 = \frac{r(1-\gamma)}{\varphi\,(2\gamma - 1)} \tag{15}$$

With the mixing length of the transition point known, the wake velocity coefficient profile of a single turbine can be obtained from the two processes as:

$$\alpha(x) = \begin{cases} \frac{\gamma}{1+\varphi\frac{x}{r}} & \text{if } x \le x_0 \\ 1 - \frac{2(1-\gamma)}{1+\varphi\frac{x-x_0}{r}} & \text{if } x \ge x_0 \end{cases} \tag{16}$$

Using similar procedures, the wake velocity coefficient of the n^{th} turbine can be defined as:

$$\alpha(x) = \begin{cases} \frac{\gamma}{1+\varphi\frac{x}{r}}\left(1-\frac{2(1-\gamma)}{1+\varphi\frac{x_{max}-x_0}{r}}\right)^{(n-1)} \\ \text{if } x \leq x_0 \\ \left(1-\frac{2(1-\gamma)}{1+\varphi\frac{x-x_0}{r}}\right)\left(1-\frac{2(1-\gamma)}{1+\varphi\frac{x_{max}-x_0}{r}}\right)^{(n-1)} \\ \text{if } x \geq x_0 \end{cases} \tag{17}$$

At $n = 1$, Equation 17 is equal to Equation 16.

The entrainment φ is an empirical formula which has been widely utilized in wind turbine technologies. Based on [26], the entrainment constant has been determined by experiment where $\varphi = 0.04$ for offshore wind turbines, and $\varphi = 0.075$ for onshore wind turbines. Others have used an empirical formula which is dependent on the surface roughness of the site and the hub height of the turbines [23, 24]. In this study, the empirical formula has been adapted and is given as:

$$\varphi = \frac{C}{ln\left(\frac{z}{z_o}\right)} \tag{18}$$

where: z is the position/height of the centre of the turbine, z_o is the surface roughness of the site where the turbines are deployed, C is a constant. In the case of wind turbines, $C = 0.5$ however for tidal turbines this value is not expected to be the same and different value have been tested by comparing with CFD results and the value which gave better agreement was selected.

The bypass and turbine velocity coefficients are assumed constant throughout the farm and have the same effect in each of the turbines. Applying Bernoulli, continuity and momentum conservation equations between stations 11 and 14 yields the following two relations: (Refer to [3] for more detailed derivations).

$$\left(1-\left(\frac{B\gamma}{\alpha_{min}}+\frac{1-B\gamma}{\beta}\right)\right) = \frac{u^2}{2gh}\left(\beta^2-1\right) \tag{19}$$

$$\gamma = \frac{2\left(\beta+\alpha_{min}\right)-\frac{\left(\beta-1\right)^3}{B\beta\left(\beta-\alpha_{min}\right)}}{4+\frac{(\beta^2-1)}{\alpha_{min}\beta}} \tag{20}$$

Combining Equations 19 and 20, a quadratic equation definition for the bypass velocity coefficient can be formulated as:

$$\begin{aligned} \frac{F_r^2}{2}\beta^4 + 2\alpha_{min}F_r^2\beta^3 - \left(2-2B+F_r^2\right)\beta^2 \\ - \left(4\alpha_{min}+2\alpha_{min}F_r^2-4\right)\beta \\ + \left(\frac{F_r^2}{2}+4\alpha_{min}-2B\alpha_{min}^2-2\right) = 0 \end{aligned} \tag{21}$$

where: $F_r = \frac{u}{\sqrt{gh}}$ is the upstream Froude number, and B is the blockage ratio. The blockage ratio is equal to the ratio of the sum of the area of turbines in the same row (A_{total}) to the cross-sectional area of the channel ($B = A_{total}/bh$). Solving for the bypass velocity coefficient enables us to calculate all the other velocity coefficients and the power extraction from a tidal stream farm.

2) Mathematical Formulation of Power Extraction: The flow given in Fig. 1 has been analysed considering the assumptions outlined in the previous section and based on the principles used by [3]. Bernoulli's equation is not valid across each turbine but it can be applied from far field toward the turbines to obtain the head difference due to the discontinuity by the turbines.

The analytical modelling starts with a single turbine and is then expanded to a tidal stream farm containing two rows of turbines by a subsequent coupling of the inlet and outlet conditions. The side effects have been taken into consideration through the bypass velocity coefficient in order to incorporate a transverse array of turbines (span-wise direction). This building process brings the idea of creating a tidal stream farm containing ideally hundreds of turbines in the stream-wise and span-wise directions taking into consideration the impact of turbine to turbine interactions on their performance. The development of the parametrised analytic models has been based on the labels and parameters given in Fig. 1.

The analytical models developed by [3] for a single row of turbines have been directly adapted as summarised below. Applying Bernoulli's equations in the fluid flow along the turbine tube between stations 11 and 12 gives:

$$h + \frac{1}{2g}u^2 = h_{12t} + \frac{1}{2g}u^2\gamma^2 \tag{22}$$

similarly, the Bernoulli's equation between stations 13 and 14 is given as:

$$h_{13t} + \frac{1}{2g}u^2\gamma^2 = h_{14} + \frac{1}{2g}u^2\alpha_{min}^2 \tag{23}$$

Combining Equations 22 and 23, the head difference at station 11 and 14 is defined as:

$$h - h_{14} = h_{12t} - h_{13t} + \frac{1}{2g}u^2\left(\alpha_{min}^2-1\right) \tag{24}$$

Applying Bernoulli in the bypass flow between stations 11 and 14 gives:

$$h + \frac{1}{2g}u^2 = h_{14} + \frac{1}{2g}u^2\beta^2 \tag{25}$$

Re-arranging Equation 25, the head difference between stations 11 and 14 can be written as:

$$h - h_{14} = \frac{1}{2g}u^2\left(\beta^2-1\right) \tag{26}$$

combining Equations 24 and 26, the head difference at stations 12 and 13 can be defined as:

$$h_{12t} - h_{13t} = \frac{1}{2g}u^2\left(\beta^2-\alpha_{min}^2\right) \tag{27}$$

The thrust loading F_{11} is defined by the head differences along the control volume normal to the turbine and can be written as:

$$F_{11} = \rho g\left(h_{12t} - h_{13t}\right)A_{11} \tag{28}$$

where A_{11} is the swept area of the turbine in the first row and first column. Substituting Equation 27 into Equation 28 gives the thrust loading as:

$$F_{11} = \frac{1}{2}\rho u^2 \left(\beta^2 - \alpha_{min}^2\right) A_{11} \tag{29}$$

and the power extracted by the turbine can be calculated as:

$$P_{11} = \gamma u F_{11} = \frac{1}{2}\rho u^3 \gamma \left(\beta^2 - \alpha_{min}^2\right) A_{11} \tag{30}$$

The total power extracted from the first row of turbines can be obtained by:

$$P_{row1} = m\gamma u F_{11} = m\frac{1}{2}\rho u^3 \gamma \left(\beta^2 - \alpha_{min}^2\right) A \tag{31}$$

where: A is the swept area of each turbine assuming the same size of devices in the tidal stream farm and m is the total number of turbines in the first row row. Keep in mind that the side effects in the lateral spacing are accounted for by the bypass velocity coefficient (β) in the equation.

The analytical models for a single row of turbines were expanded to include a second row of turbines taking into consideration the impact of wake interaction from the upstream turbines on the performance of downstream turbines. Using the same approach as before, applying Bernoulli's principle in the fluid flow along the turbine tube at stations 1'4 and 22 gives:

$$h_{1'4} + \frac{1}{2g}\alpha^2 u^2 = h_{22t} + \frac{1}{2g}\gamma^2 \alpha^2 u^2 \tag{32}$$

and similarly at stations 23 and 24, the Bernoulli's equations can be defined as:

$$h_{23t} + \frac{1}{2g}\gamma^2 \alpha^2 u^2 = h_{24} + \frac{1}{2g}\alpha_{min}^2 \alpha^2 u^2 \tag{33}$$

Combining Equations 32 and 33, the head difference at station 1'4 and 24 is written as:

$$h_{1'4} - h_{24} = h_{22t} - h_{23t} + \frac{1}{2g}u^2 \alpha^2 \left(\alpha_{min}^2 - 1\right) \tag{34}$$

applying Bernoulli's principle in the bypass flow between stations 1'4 and 24 gives:

$$h_{1'4} + \frac{1}{2g}\beta'^2 u^2 = h_{24} + \frac{1}{2g}\beta^2 \beta'^2 u^2 \tag{35}$$

where: $1 \leq \beta' < \beta$. Re-arranging Equation 35, the head difference between stations 1'4 and 24 can be written as:

$$h_{1'4} - h_{24} = \frac{1}{2g}u^2 \beta'^2 \left(\beta^2 - 1\right) \tag{36}$$

combining Equations 34 and 36, the head difference at stations 22 and 23 can be defined as:

$$h_{22t} - h_{23t} = \frac{1}{2g}u^2 \left(\beta'^2(\beta^2 - 1) - \alpha^2(\alpha_{min}^2 - 1)\right) \tag{37}$$

The thrust loading F_{21} can be defined by the head difference at stations 22 and 23 as:

$$F_{21} = \rho g \left(h_{22t} - h_{23t}\right) A_{21} \tag{38}$$

where A_{21} is the swept area of the turbine in the second row and first column. Substituting Equation 37 into Equation 38, the thrust loading can be defined as:

$$F_{21} = \frac{1}{2}\rho u^2 \left(\beta'^2(\beta^2 - 1) - \alpha^2(\alpha_{min}^2 - 1)\right) A_{21} \tag{39}$$

and the power extracted by the turbine can be calculated as:

$$P_{21} = \gamma u F_{21} = \frac{1}{2}\rho u^3 \gamma \left(\beta'^2(\beta^2 - 1) - \alpha^2(\alpha_{min}^2 - 1)\right) A_{21} \tag{40}$$

The total power extracted by the second row of turbines can be then calculated considering the number of turbines in the spanwise direction as:

$$P_{row2} = m\left(\frac{1}{2}\rho u^3 \gamma \left(\beta'^2(\beta^2 - 1) - \alpha^2(\alpha_{min}^2 - 1)\right) A\right) \tag{41}$$

The power coefficient (C_p) of a single turbine from the second row can be extracted from Equation 41 and is defined as:

$$C_p = \gamma \left(\beta'^2(\beta^2 - 1) - \alpha^2(\alpha_{min}^2 - 1)\right) \tag{42}$$

The influence of wake interaction is accounted for by the α function discussed previously by varying the spacing between the rows of turbines. The velocity coefficient β' is unknown and the results from a series of CFD simulations have been used to estimate this value in order to reduce the number of parameters involved in the analytical building process. The formulation of the analytical models so far have been limited for the power extraction from ideally hundreds of columns and two rows of turbines however a further work will focus on expanding these models to include for hundreds of rows of turbines.

B. CFD modelling

Most researchers accept that simple momentum sink zone models such as the actuator disc methods are crude and make it difficult to incorporate energy loss processes. However, they are one of the few computationally realistic approaches for gaining insight into the behaviour of substantial clusters of devices. This study builds upon this accepted methodology by incorporating additional geometric features that induce energy absorption from the flow which also lead to a downstream wake structure intended to reflect more closely those of the real turbines than simple momentum sink zone models. In this study, a different tidal turbine modelling method called *Immersed Body Force (IBF)* is employed. This IBF model have been used to investigate different issues of the MRL turbine as documented by [14, 27].

For the IBF approach, a forcing function per unit volume of the blades (F_b) representing the resistance by the turbine against the flow is used to create momentum change. The force function was imposed in the NS equations and a code was developed by considering drag (F_{RD}) and lift (F_{RL}) resistance forces applied by the blades on the fluid flow as shown in Fig. 5.

The force applied by the vertical blade was considered entirely as a drag resistance force while the other two blades

have both drag and lift resistance forces. The forcing function can be defined as:

$$\overline{F}_b = \overline{F}_{RD} + \overline{F}_{RL} \tag{43}$$

The IBF model comprises two parts:

1) A set of resistance forces seated on the cells corresponding to the fixed blade positions.
2) A force ring designed to represent the effect of the main turbine vortex as shown in Fig. 5.

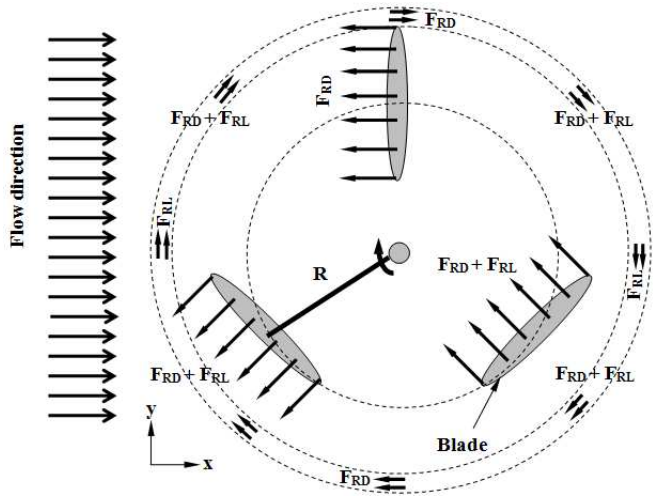

Fig. 5: Illustration of body forces applied by each blade and annular section

The parameters (F_{RD} and F_{RL}) represent the associated resistances against the incoming flow. This type of representation has several advantages as summarised below:

- It reduces the requirement of mesh resolution at the surface because there is no physical presence of the blades in the model, which minimises the requirement of fine meshing to treat the blade surface and fluid interaction.
- It is applied in a volume which creates complex motions within the turbine housing
- The geometric features lead to downstream wake structures intended to reflect more closely those of the real turbines.
- It allows application of both drag and lift resistances against the flow based on the blade position.

The resistance force is the input parameter required in the IBF modelling approach. This resistance force can be used to calibrate the energy extraction which inevitably depends upon the inflow conditions. Given that the turbines interact with each other these inlet conditions are themselves unknown at the start of the calculation which makes it difficult to apply the correct resistance force to each of the downstream row of turbines. However, due to the downstream turbine operating on the wake of upstream turbines, the resistance force applied to the downstream turbines should be different and it was reduced arbitrarily by 10% from the resistance force of the upstream turbine.

In most of the actuator disc methods, the turbine is modelled using a porous disc that provides axial resistance coefficient, K_L, to the incoming flow. The thrust force is related to the dynamic head at the disc using the axial resistance coefficient, sometimes called the loss factor, as:

$$T = K_L \frac{1}{2} \rho A \overline{u_t^2} \tag{44}$$

where, A is the projected area of the turbine and $\overline{u_t}$ is the streamwise average velocity normal to the disc. The power removed from the flow by the presence of the device is therefore defined using the thrust force and the average velocity as:

$$P = T\overline{u_t} \tag{45}$$

Equation 44 has been used to calculate the thrust force by several researchers working on tidal turbines as documented in [28–31]. The thrust coefficient, C_T, is defined using the thrust experienced by the turbine and the thrust force available in the upstream flow as:

$$C_T = \frac{T}{\frac{1}{2}\rho A u_\infty^2} \tag{46}$$

Similarly, the power coefficient, C_P, can be defined using the power removed from the flow by the device and the kinetic flux available in the upstream flow as:

$$C_P = \frac{P}{\frac{1}{2}\rho A u_\infty^3} \tag{47}$$

The operating point of the MRL turbine is obtained by varying the value of F_b. Thus an empirical relationship between the resistance force, F_b, and the resistance coefficient, K_L , has been established as shown in Equation 48 in order to employ Equation 47 for the calculation of the performance of individual turbines in the farm.

$$K_L = 0.48e^{0.187F_b} \tag{48}$$

The formulation of this relationship is important as the equations used to calculate the performance of the turbine are developed based on the resistance coefficient, K_L, while the IBF model is developed based on the resistance force, F_b. This relationship was established using a detailed calculation of the power coefficients of a single turbine using conservation of linear momentum approach.

1) Computational set-up: The domain size extends 51D (10.2 m) longitudinal distance, 25.3D (5.06 m) laterally and with an overall height of 10.3125D (2.0625 m). The initial conditions for the simulation were $\alpha = 1$ up to 7.3125D, $\alpha = 0$ above this level, representing a water level of 7.3125D from the ground with the rest of the domain occupied by air. Two phases were used as the simulation was carried out with a free surface using volume of fluid (VOF) interface tracking method.

The turbine has an overall diameter of D = 0.20 m and a length of L = 0.22 m. The blades have maximum thickness and chord length of 1.7 cm and 9.5 cm respectively and the same size of turbines have been used in the farm. These turbines were positioned 2D below the free surface.

Large Eddy Simulation (LES) modelling technique was used for the CFD calculation. The sub-grid scale stresses were modelled using one-equation eddy viscosity model which is commonly used in the simulation of turbulent flows. The OpenFOAM finite volume CFD code software package was employed to perform the simulations. The $1/7^{th}$ power law velocity profile, which is an approximate tidal velocity profile developed by assuming a power law, was used for the inlet and a buoyant pressure boundary condition was used for both the inlet and outlet of the computational domain.

III. Results and Discussions

A. Flow Field Analysis

Fig. 6 shows the velocity contours of two rows and single column turbine configuration. The longitudinal spacing between the turbines (rows) is 20D. It is clear from the velocity contour that there is a huge interaction of the wake of upstream turbine with the downstream turbine which has a direct impact on the performance of the downstream turbine.

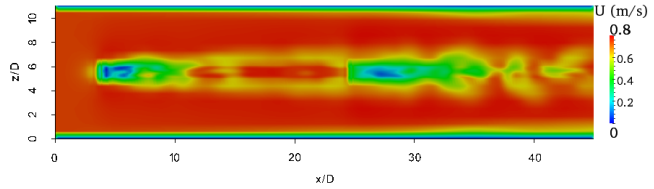

Fig. 6: Velocity contours of two turbine configurations

A small tidal farm containing six turbines based on the turbine configuration given in Fig. 1 was constructed to investigate the blockage effect on the flow field and performance of individual turbines. Fig. 7 shows the velocity contour of six turbines configured in two rows and three columns. The longitudinal spacing between the rows is 15D while the lateral spacing between the turbines is 6D. The wake of the upstream row of turbines interacts with the downstream row of turbines which affects the performance of the downstream rows.

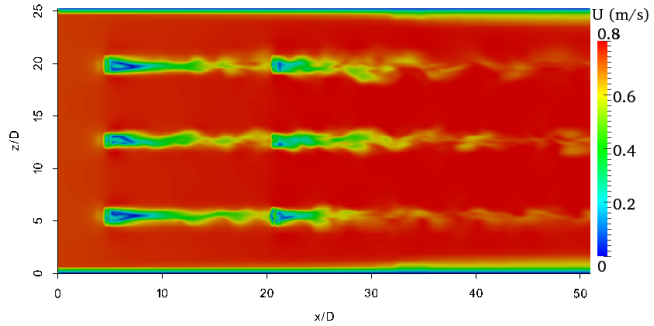

Fig. 7: Velocity contours of regularly configured six turbine simulations

The wake interaction can be minimised by using off-set turbine configurations, which could improve the cumulative power extraction by utilising the accelerated flow regions observed due to the venturi flow created by the presence of turbines in the spanwise direction. However, this requires appropriate lateral spacing based on the size of the turbines to avoid the wake interaction between the turbines in the spanwise direction. The wake interaction can also be avoided by increasing the longitudinal spacing although there is always space constraint which needs to be optimised.

To obtain a clear picture of the velocity profile, a one-dimensional velocity dataset was extracted along the stream direction through the centre of the turbines in column 2 from Fig. 7. Fig. 8 shows comparison of the wake velocity profiles calculated using both the analytical and CFD models. A discontinuity of the velocity profile on the upstream of each row can be observed for the analytical result. The main reason is that the analytical velocity wake profile model is developed for the wake regions of each turbine or row and it only extends up to the local incident region of each downstream turbine.

The CFD model result has faster convergence immediately downstream of the turbine (near turbine region) compared to the analytic model calculated with the constant value, $C = 1.5$, in both rows. The results from the analytic wake model in the near turbine region can be increased its convergence with an increase of the constant value, C, which gives the possibility of good agreement with the CFD result. However, estimating the wake velocity coefficient in the near turbine region may not be as important as the one in the recovering region because it is obvious that turbines could not be employed as close as the near turbine region as the flow is significantly affected by the upstream turbine though it is good to have full picture of the velocity profile on the whole mixing region.

The velocity profile in the recovering region calculated with the constant value, $C = 1.5$, showed faster wake recovery between 6D and 15D but showed good agreement around the local incident region of the second row. However, the wake recovery of the velocity in the wake region of the second row showed small difference between 21D and 26D with the velocity profile from the CFD result showed higher value from 26D onwards. The constant value C has huge impact on the calculation of the velocity profile using the analytical model and changing its value can minimise the differences observed with the CFD result. Thus careful selection of this constant value is important and future work will focus on experimental works to obtain universally applicable value for tidal turbines based on the experiences from the wind turbine technologies.

Defining the wake velocity profile model using the spacing (mixing length scale) between rows of turbines has significant impact on the calculation of power extraction from tidal stream farms because of the greater freedom that gives to vary the spacing in order to minimise the influence of wake interaction on the performance of downstream turbines. It also provides a potential option of using these wake models as an input function for optimisation of the location of the devices for a higher power extraction.

B. Power Analysis

The power extraction of the two turbines configured in a single column at 20D turbine spacing (Fig. 6) was calculated

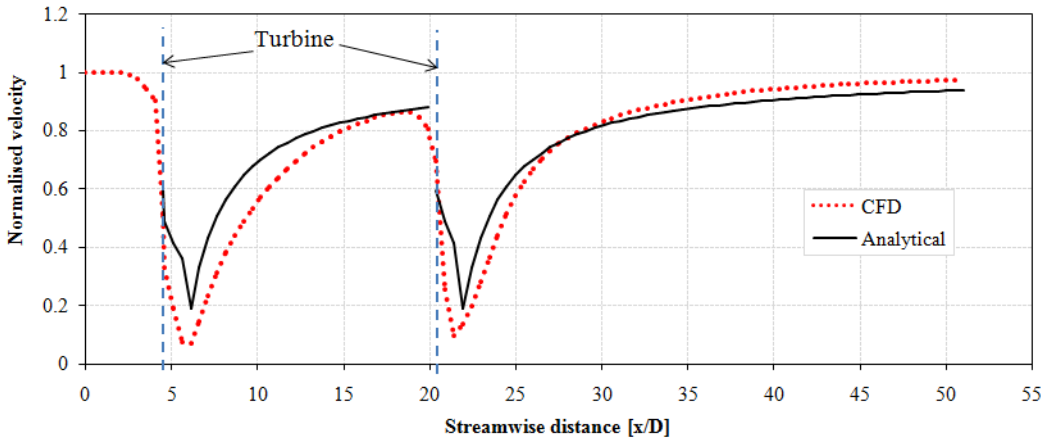

Fig. 8: Comparison of velocity profiles through the centre of one column of turbines

using both the analytic and CFD models. The power extracted by the upstream turbine showed almost the same value by both models but slightly less than the power from an isolated turbine which may be affected by the blockage of downstream turbine. However, the power extracted by the downstream turbine is much lower than the power extracted by an isolated turbine. This is an indication that the given turbine spacing is not enough to avoid the wake interaction that affects the performance of the downstream turbine. Note that all the power extraction discussed in this study are excluding the power loss during re-mixing in the wake regions. This analysis showed that more than 91% of the performance of an isolated turbine can be achieved from any downstream turbines spaced 20D apart in the streamwise direction.

Comparison of the power extraction using both the analytical and CFD models from two rows and three columns of turbines is shown in Fig. 9. Note that the results of one column of turbines are shown from the analytical model because of similar values for the other columns of turbines. The result clearly shows that the downstream turbines are experiencing massive energy shadowing from the upstream turbines due to the wake interaction that affects the local incident velocity resulting in a low power extraction from the downstream turbines. Unlike the results from the single column turbine configurations, the results from the analytical model appears to be lower than the CFD model in both rows of turbines.

There is also an indication that the power extraction from individual turbines in the same row from the CFD model is different in contrary to the results from the analytical model. This is purely because of the blockage effect which is probably not well captured by the analytical model. Thus a further improvement of the analytical models is required in future studies in order to minimise these differences.

IV. Conclusion

Analytic models have been developed to describe the flow profiles downstream of the turbines and to estimate the total power extraction of a tidal stream farm containing two rows and three columns of turbines. The results discussed in this

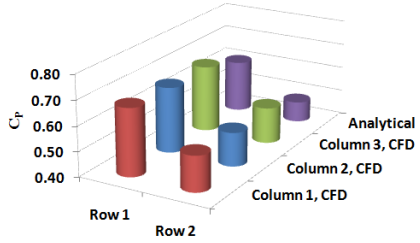

	Row 1	Row 2
Column 1, CFD	0.672	0.543
Column 2, CFD	0.665	0.535
Column 3, CFD	0.668	0.544
Analytical	0.609	0.482

Fig. 9: Comparison of power coefficients of the individual turbines calculated using both modelling methods

paper are from an early stage project work which is mainly focused on optimisation of tidal stream farms and more future works are certainly required in order to improve fidelity of the developed models and on expanding the model to include several rows of turbines.

The developed models showed the capability of examining the wake velocity profiles and estimating the performance of arrays of turbines taking in to consideration the influence of wake interactions. A small longitudinal spacing between turbines inflicted a massive energy shadowing that affects the performance of downstream turbines. Based on the analysis of the influence of wake interaction, more than 91% of the performance of an isolated turbine can be achieved with turbines spaced 20D apart. In addition, comparison of the wake velocity profiles and the power extraction calculated using both the analytic and CFD models showed reasonable agreement.

Acknowledgement

This research was funded by the Engineering and Physical Sciences Research Council (EPSRC) under the SuperGen Marine research programme.

REFERENCES

[1] C. Garrett and P. Cummins. The efficiency of a turbine in a tidal channel. *Journal of Fluid Mechanics*, 588:243–251, 2007.

[2] JI Whelan, JMR Graham, and J. Peiro. A free-surface and blockage correction for tidal turbines. *Journal of Fluid Mechanics*, 624:281–291, 2009.

[3] GT Houlsby, S. Draper, and MLG Oldfield. Application of linear momentum actuator disc theory to open channel flow. Technical report, Technical Report 2296-08, OUEL, 2008.

[4] Y. Li, J.L. Barbara, and M.C. Sander. Modeling tidal turbine farm with vertical axis tidal current turbines. In *Systems, Man and Cybernetics, 2007. ISIC. IEEE International Conference on*, pages 697–702. IEEE, 2007.

[5] R. Vennell. The energetics of large tidal turbine arrays. *Renewable Energy*, 48:210–219, 2012.

[6] R. Vennell. Estimating the power potential of tidal currents and the impact of power extraction on flow speeds. *Renewable Energy*, 36(12):3558–3565, 2011.

[7] M. Shives and C. Crawford. Overall efficiency of ducted tidal current turbines. 2010.

[8] T. Nishino and R.H.J. Willden. The efficiency of an array of tidal turbines partially blocking a wide channel. *Journal of Fluid Mechanics*, 708:596, 2012.

[9] AS Bahaj and LE Myers. Fundamentals applicable to the utilisation of marine current turbines for energy production. *Renewable energy*, 28(14):2205–2211, 2003.

[10] AJ Williams, TN Croft, I. Masters, MR Willis, and M. Cross. Combined BEM-CFD modelling of tidal stream turbines using site data. In *International Conference on Renewable Energies and Power Quality (ICREPQ10)*, 2010.

[11] C. Jo, J. Yim, K. Lee, and Y. Rho. Performance of horizontal axis tidal current turbine by blade configuration. *Renewable Energy*, 42:195–206, 2012.

[12] ME Harrison, WMJ Batten, and AS Bahaj. A blade element actuator disc approach applied to tidal stream turbines. In *OCEANS 2010*, pages 1–8. IEEE, 2010.

[13] L. Bai, R.R.G. Spence, and G. Dudziak. Investigation of the influence of array arrangement and spacing on tidal energy converter (TEC) performance using a 3-dimensional CFD model. In *Proceedings of the 8th European Wave and Tidal Energy Conference, Uppsala, Sweden*, 2009.

[14] M.G. Gebreslassie, G.R. Tabor, and M.R. Belmont. Numerical simulation of a new type of cross flow tidal turbine using openfoam–part ii: Investigation of turbine-to-turbine interaction. *Renewable Energy*, 50:1005–1013, 2013.

[15] WMJ Batten and AS Bahaj. CFD simulation of a small farm of horizontal axis marine current turbines. In *Proceedings World Renewable Energy Congress WREC IX*. Elsevier Science, 2006.

[16] LE Myers, B. Keogh, and AS Bahaj. Experimental investigation of inter-array wake properties in early tidal turbine arrays. In *OCEANS 2011*, pages 1–8. IEEE, 2011.

[17] T. Daly, L.E. Myers, and A.B.S. Bahaj. Experimental investigation of the effects of the presence and operation of tidal turbine arrays in a split tidal channel. *Volume 9 Marine and Ocean Technology*, page 2262, 2011.

[18] Chul Hee Jo, Kang H Lee, Jun H Lee, and Cristian Nichita. Multi-arrayed tidal current energy farm and the integration method of the power transportation. In *Power Electronics, Electrical Drives, Automation and Motion (SPEEDAM), 2012 International Symposium on*, pages 1428–1431. IEEE, 2012.

[19] A. Betz. Das Maximum der theoretisch moglichen Ausnutzung des Windes durch Windmotoren. *Zeitschrift fur das gesamte Turbinenwesen*, 26:307–309, 1920.

[20] L. Myers and AS Bahaj. Wake studies of a 1/30th scale horizontal axis marine current turbine. *Ocean Engineering*, 34(5-6):758–762, 2007.

[21] FW Lanchester. A contribution to the theory of propulsion and the screw propeller. *Journal of the American Society for Naval Engineers*, 27(2):509–510, 1915.

[22] S. Frandsen, R. Barthelmie, S. Pryor, O. Rathmann, S. Larsen, J. Højstrup, and M. Thøgersen. Analytical modelling of wind speed deficit in large offshore wind farms. *Wind Energy*, 9(1-2):39–53, 2006.

[23] N.O. Jensen. *A note on wind generator interaction*. Risø National Laboratory, 1983.

[24] I. Katic, J. Højstrup, and NO Jensen. A simple model for cluster efficiency. *European Wind Energy Association*, pages 407–409, 1986.

[25] T. Ishihara, A. Yamaguchi, and Y. Fujino. Development of a new wake model based on a wind tunnel experiment. *Global Wind Power*, 2004.

[26] J.F. Manwell, J.G. McGowan, and A.L. Rogers. Wind energy explained: theory, design and application. 2002. *John Wiley&Sons Ltd, UK*, page 577, 2002.

[27] M.G. Gebreslassie, G.R. Tabor, and M.R. Belmont. CFD simulations for sensitivity analysis of different parameters to the wake characteristics of tidal turbine. *Open Journal of Fluid Dynamics*, 2(3):56–64, 2012.

[28] J. Giles, L. Myers, A.B. Bahaj, and B. Shelmerdine. The downstream wake response of marine current energy converters operating in shallow tidal flows. 2011.

[29] X. Sun. Numerical and experimental investigation of tidal current energy extraction. 2008.

[30] ME Harrison, WMJ Batten, LE Myers, and AS Bahaj. Comparison between CFD simulations and experiments for predicting the far wake of horizontal axis tidal turbines. *Renewable Power Generation, IET*, 4(6):613–627, 2010.

[31] C.S.K. Belloni and R.H.J. Willden. Flow field and performance analysis of bidirectional and open-centre ducted tidal turbines. In *9th European Wave and Tidal Energy Conference*, 2011.